

Optimization of empirical typhoon model considering the difference of radius between pressure gradient and wind speed distributions

Masaya Toyoda, Nobuhito Mori & Jun Yoshino

To cite this article: Masaya Toyoda, Nobuhito Mori & Jun Yoshino (2022): Optimization of empirical typhoon model considering the difference of radius between pressure gradient and wind speed distributions, Coastal Engineering Journal, DOI: [10.1080/21664250.2022.2035514](https://doi.org/10.1080/21664250.2022.2035514)

To link to this article: <https://doi.org/10.1080/21664250.2022.2035514>



© 2022 The Author(s). Published by Informa UK Limited, trading as Taylor & Francis Group.



Published online: 06 Feb 2022.



Submit your article to this journal [↗](#)



Article views: 79





View related articles [↗](#)



View Crossmark data [↗](#)

Optimization of empirical typhoon model considering the difference of radius between pressure gradient and wind speed distributions

Masaya Toyoda ^a, Nobuhito Mori ^{b,c} and Jun Yoshino^d

^aDepartment of Architecture and Civil Engineering, Toyohashi University of Technology, Aichi, JAPAN; ^bDisaster Prevention Research Institute, Kyoto University, Kyoto, Japan; ^cSchool of Engineering, Swansea University, Swansea, UK; ^dDepartment of Civil Engineering, Faculty of Engineering, Gifu University, Gifu, Japan

ABSTRACT

This study proposes empirical relations for the ratio of the radius of maximum pressure gradient to the radius of maximum wind speed for the empirical typhoon model (ETM) based on the results of analysis of multiple typhoons obtained from the meteorological model. One proposed relation was parameterized based on the attenuation rate from the peak time to landfall time. The other was parameterized based on the distance from where the typhoon reached its peak intensity to the coastline. These relationships are useful for practical applications. In addition, the typhoon pressure shape parameter B was calculated from the constructed equations and the relational equation proposed by Holland. The improvement in accuracy, as compared with conventional ETM ($B = 1$, and B estimated by the gradient-wind equilibrium assumption), was determined for three cases of typhoons making landfall in Japan in recent years. As a result, it was confirmed that the proposed equations for parameter B are the most accurate amongst the three estimation methods. Accordingly, the improvement in the accuracy of the ETM using the estimation equations was validated. When using the ETM in the future, high accuracy can be realized by utilizing the estimation equations used in this study.

ARTICLE HISTORY

Received 3 August 2021
Accepted 25 January 2022

KEYWORDS

Empirical typhoon model; radius ratio; radius of maximum wind speed; radius of maximum pressure gradient; storm surge

1. Introduction

Accurate estimation of atmospheric pressure drops and strong winds associated with tropical cyclones (TCs) leads to improved accuracy of severe TC-related coastal disaster estimation. In recent years, numerical modeling using regional climate models or atmosphere-ocean coupled models that can simulate typhoons, related waves, and storm surges has been increasingly used due to the expansion of computing power (Mori et al. 2014). For example, Mori et al. (2014) conducted numerical experiments for typhoon Haiyan in 2013 to investigate the characteristics of local storm surge amplification in the Leyte Gulf and Tacloban areas. This study used two types of meteorological models with 1-km resolution: the Weather Research and Forecasting model (Skamarock et al. 2008; the Cloud Resolving Storm Simulator, Tuboki and Sakakibara 2002) and the storm surge model. Accordingly, Haiyan and its related severe storm surges were simulated with high accuracy. In addition, they reported that the seiche of the Leyte Gulf enhanced the storm surge, and the storm surge in the Leyte Gulf could potentially be amplified by a particular typhoon track.

The use of atmosphere-ocean coupled models for typhoon-induced storm surges is becoming prominent. However, hazard maps, countermeasures, and many typhoon disaster assessments for storm surges

are widely at the policy level in the parameterized empirical typhoon model (ETM) and storm surge model in Japan (Ministry of Land, Infrastructure, Transport and Tourism, Japan 2020). Empirical methods for estimating typhoon meteorological fields have been proposed in many studies (Schloemer 1954; Myers 1954; Holland 1980; Fujii and Mitsuta 1986; Chavas, Lin, and Emanuel 2015; Wang et al. 2015). Fujii and Mitsuta (1986) and Chavas, Lin, and Emanuel (2015) estimated the wind speed distribution. Holland (1980) and Wang et al. (2015) proposed estimation methods for pressure and wind speed distributions. The methods proposed by Schloemer (1954) and Holland (1980) are widely used because of the small number of input variables and the simplicity of the equations. Although various other ETMs have been proposed by many researchers (Jelesnianski, Chen, and Shaffer 1992; Willoughby, Darling, and Rahn 2006), this study targets the ETM proposed by Schloemer (1954) and used by Holland (1980) and Fujii and Mitsuta (1986). The ETM is widely used as a general method in coastal engineering in Japan. Therefore, this study focuses on the practical use by policymakers and port managers in Japan. In addition, owing to the low computation cost and ease of handling, the ETM

(Holland 1980; Fujii and Mitsuta 1986) has been widely employed for estimating meteorological fields using simplified typhoon information (e.g. minimum central pressure) for storm surges. Therefore, engineers and policymakers are likely to adopt ETM. The following equations express the ETM for pressure (Myers 1954) and wind speed distribution (Fujii and Mitsuta 1986).

$$P(r) = P_c + \Delta P \exp\left(-\frac{1}{x^B}\right) \quad (1)$$

$$V(r) = -\left(\frac{rf}{2}\right) + \sqrt{\left(\frac{rf}{2}\right)^2 + \frac{\Delta P B}{\rho_a x^B} \exp\left(-\frac{1}{x^B}\right)} \quad (2)$$

where $P(r)$ [hPa] is the pressure at a point r km from the typhoon center, P_c [hPa] is the central pressure of the typhoon, and ΔP [hPa] is the pressure depression from the atmospheric environmental pressure (here, we use $1013\text{hPa} - P_c$), x is expressed as the ratio between the distance r [km] and the radius of maximum wind speed R_w [km] ($x = r/R_w$). In the wind speed equation, $V(r)$ [m/s] is the wind speed, ρ_a [g/m³] is the atmospheric density, and f [rad/s] is the Coriolis parameter ($2 \times 7.29 \times 10^{-5} \times \sin\phi$), and ϕ [rad] is the latitude. Equation (1) expresses the barometric pressure distribution, and Equation (2) expresses the wind speed distribution as a function of ΔP , r , and R_w . Both equations are based on the study conducted by Schloemer (1954). The coefficient B appears in both atmospheric pressure and wind speed distributions as a scaling parameter, and $B = 1$ is empirically proposed by Myers (1954) and Fujii and Mitsuta (1986). Furthermore, it is necessary to consider the effect of typhoon movement and friction on the wind speed in Equation (2). Blaton's equation is widely used to evaluate the effects of typhoon movement.

$$\frac{1}{r_t} = \frac{1}{r} + \frac{1}{V(r)} \frac{\partial \psi}{\partial t} \quad (3)$$

where t indicates time, r_t is the radius of curvature of the streamline at t , and ψ indicates the particle traveling direction. This equation indicates that stronger winds blow on the right side of the direction of typhoon movement. The wind speed considering the effect of movement can be obtained from Equations (2) and (3), respectively. In addition, considering the ground surface friction, the surface wind speed was estimated by multiplying the wind speed reduction coefficient $C(x)$ according to the super gradient wind method proposed by Fujii and Mitsuta (1986).

$$C(x) = C(\infty) + [C(x_p) - C(\infty)] \left(\frac{x}{x_p}\right)^{k-1} \times \exp\left\{\left(1 - \frac{1}{k}\right) \left[1 - \left(\frac{x}{x_p}\right)^k\right]\right\}, \quad (4)$$

where $x = r/R_w$, x_p is the value of x that maximizes $C(x)$, k is the parameter corresponding to the shape of the typhoon, and $C(\infty)$ is $C(x)$ at infinity from the

typhoon. Here, x_p is set to 0.5, k is set to 2.5, $C(\infty)$ is set to 2/3, and $C(x_p)$ is set to 1.2 empirically. These values are the same as those reported in previous studies (Matoba, Murakami, and Shibaki 2006; Yamaguchi et al. 2012). The current ETM calculates atmospheric pressure using Equation (1), and the wind speed by Equations (2) to (4). This ETM is widely used for the assumption of storm surge inundation in Japan (Kawasaki et al. 2016; Shibutani et al. 2017). However, the setting of $B = 1$ is still adopted.

A well-known problem in ETMs is a large error in pressure and wind speed estimated in an approaching typhoon relative to actual observations (Murakami, Yasuda, and Yoshino 2007). This could be attributed to the fixed-parameter B generally adopted for all typhoons. The relational equation is as follows (Holland 1980):

$$\frac{R_p}{R_w} = \left[\frac{B}{(B+1)}\right]^{\frac{1}{B}} \quad (5)$$

where R_p [km] is the distance from the center of the typhoon to the point with the maximum pressure gradient. R_w [km] indicates the distance from the typhoon center to the point with the maximum wind speed. Equation (5), as shown in Equations (1) and (2), are also based on the equation proposed by Schloemer (1954) that is a relation proposed by Holland (1980) using a scaling parameter. Equation (5) shows that parameter B is related to R_p and R_w . These factors are not constant and need to be changed according to the structure of the typhoon (Holland 1980; Hubbert et al. 1991). Holland (1980) constructed the equation for B as follows:

$$B = \rho_a e V_{max}^2 / \Delta P \quad (6)$$

Here, e is the base of natural logarithms. This equation assumes the gradient–wind equilibrium and considers the surface friction and moving speed of the TC. Therefore, it is inferred that the distribution is not suitable at the time of landfall. Figure 1 shows an example of the cross-sectional atmospheric pressure distribution for different values of B . The horizontal axis represents the distance from the center, and the vertical axis represents the atmospheric pressure. A large difference can be observed in the pressure distribution depending on the setting of B . In the case of a small B value (< 1.0), the pressure gradient until the typhoon approaches becomes gradual, and near the center of the typhoon, the pressure gradient becomes steep. In the case of a large B value (> 1.0), the opposite tendency is observed.

Equation (5) shows that if the ratio of R_p and R_w (radius ratio; R_p/R_w) can be estimated, it is possible to calculate parameter B backward. However, it is generally difficult to use R_p/R_w because the values of R_p and R_w are not obtained. Estimates of R_w are available from satellites and equations for some of the best tracks. However, R_w is not included in the best track of the JMA best track. In addition, no estimation was disclosed for R_p . In addition,

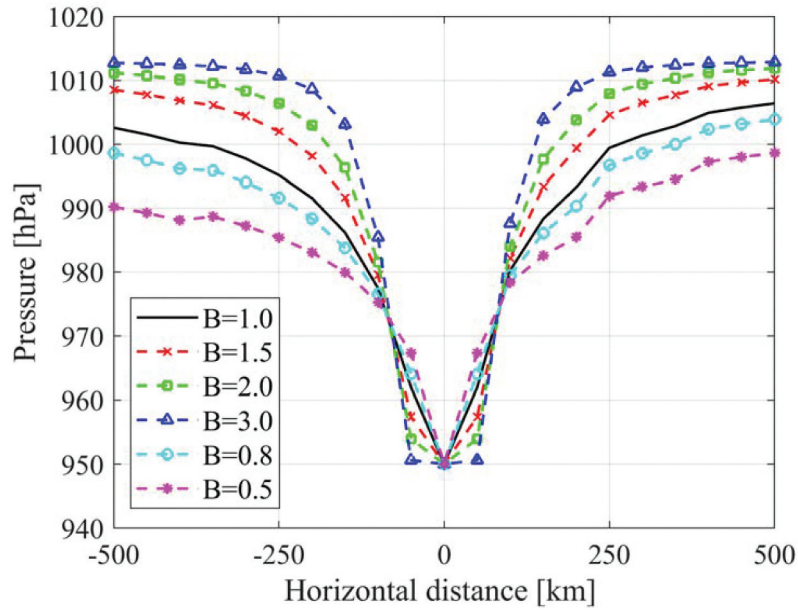


Figure 1. The example of pressure distribution within a radius of 500 km from the center of the typhoon. Each line color uses a different B value. The black line is $B = 1$, the red one is $B = 1.5$, the green one is $B = 2.0$, the blue one is $B = 3.0$, the light blue one is $B = 0.8$, and the pink one is $B = 0.5$.

a few studies have investigated the relationship between TC characteristics. For example, Vickery and Wadhera (2008) analyzed TCs in the Atlantic and found that B has a strong negative correlation with R_w . Additionally, B has a positive correlation with the TC intensity. However, they also reported that the estimation equation for B changes depending on the target area. Therefore, it is necessary to have an appropriate relation of B based on the typhoon characteristics.

The study proposes a simplified estimation equation for R_p/R_w . Furthermore, we confirm whether the accuracy of the ETM can be improved by calculating parameter B backward using the proposed estimation equation. Additionally, the estimation equation aims to make it practically available to port managers based on the use of only the parameter that can be easily obtained even before the approach of typhoons. We conducted hindcast experiments on a large number of typhoons that had landfall in Japan between 2000 and 2017. By analyzing the R_p and R_w of the simulated typhoons in this database, an estimation equation for B is proposed.

This remainder of the paper is structured as follows: Section 2 presents the computational method used in this study; Section 3 presents the results of the analysis of 49 typhoons, in which we check the distribution of R_p/R_w and discuss the related typhoon parameters. Section 4 presents the estimation equations based on the discussion results in Section 3. In addition, validation was performed based on the recent typhoon cases (Jebi, Faxai, and Hagibis); Section 5 concludes this study and discusses future work.

2. Computational method

In a previous study conducted by the authors (Toyoda, Yoshino, and Kobayashi 2018), hindcast experiments and accuracy validation were conducted on 49 typhoons – the target of this study. These 49 typhoon landfall cases in the Pacific coast of Japan correspond to the period 2000–2017. In this study, we analyze the R_p and R_w of 49 typhoons using the hindcast simulation results. The atmospheric model is based on the Pennsylvania (PSU)/National Center for Atmospheric Research (NCAR) mesoscale model (MM5; Dudhia 1993) that is a three-dimensional, non-hydrostatic, fully compressible, cloud-resolving atmospheric model used to capture mesoscale and local-scale meteorological phenomena. The automatic movable nesting technique is introduced to MM5 to reproduce the inner-core structure near the center of a powerful typhoon, from the genesis to decaying stages. In addition, several physical parameterizations are incorporated into the original MM5. In particular, the ocean mixed layer (Shade and Emanuel 1999; Emanuel et al. 2004), dissipative heating (Bister et al. 1998; Zhang and Altschuler 1999), and sea-spray processes (Fairall, Kepert, and Holland 1994; Wang, Kepert, and Holland 2001) have been implemented to express the practical typhoon intensity and structural characteristics accurately.

According to the validation of the wind speed of typhoons at the time of landfall in Japan, compared with the JMA best track, the bias error was 1.73 m/s, the RMSE was 4.74 m/s, and the correlation coefficient was 0.85; thus, the typhoon intensity at the landfall times could be reproduced by the model with high

accuracy. Detailed information on typhoon validation was provided in a previous study (Toyoda, Yoshino, and Kobayashi 2018). From the results of the hindcast experiments, R_p is the distance from the center of the typhoon to the point where the pressure gradient is maximum, and R_w is the distance from the center of the typhoon to the position of the maximum wind speed. These were extracted from the output results every 15 min with a horizontal resolution of 3 km. However, the values obtained by averaging these values over 1 h were defined as R_p and R_w because the time fluctuations were extremely large. The two radii were analyzed at the peak times and landfall times. The results obtained by Toyoda, Yoshino, and Kobayashi (2018) are included in both the present climate and future climate experiments. However, the results of the present climate experiments are only used in this study. The estimation equation proposed in this study was constructed using the data on typhoon landfall in Japan. Hence, this result can be applied to typhoons at the time of landfall in Japan's main Islands only.

3. Results of analysis for 49 typhoon cases

3.1. Variability of R_p and R_w

Before discussing R_p and R_w , the relationship between R_p/R_w and B are confirmed. Figure 2 shows the relationship of R_p/R_w in Eq. (5) with the change in B . The horizontal axis shows parameter B , and the vertical axis shows R_p/R_w . The red line in the figure shows the point where $R_p/R_w = 0.5$ and $B = 1.0$, and this setting is used in the current ETM. As R_p/R_w approaches 1.0,

B increases rapidly. The ratio of R_p/R_w is sensitive to B in the range of 0.5 to 2. Therefore, small changes in B significantly impact the ratio of R_p/R_w . It is necessary to set the optimal B instead of fixing $B = 1.0$ based on the observed or modeled TCs.

Many typhoons follow the processes of genesis (formation), intensification, maturity, and decay stages (including extratropical transition and dissipation). The maximum wind speed and R_w are generally following the conservation law of angular momentum, and R_w tends to become smaller during the mature stage and larger during the decay stage. Furthermore, the pressure distribution also changes significantly between the mature and decay stages. Therefore, it is inferred that R_p/R_w changes with the typhoon lifetime. In this section, the R_p/R_w of the typhoon at the peak and at the time of landfall are analyzed in detail. In addition, many typhoons change to extratropical cyclones with disintegrating structures. Hence, the relationship between R_p/R_w for extratropical cyclone cases is also analyzed. This analysis aims to clarify the relationship between changes in R_p/R_w and the life of a typhoon.

This section discusses the characteristics of R_p/R_w for the simulated 49 typhoon landfall cases in Japan from 2000 to 2017, as shown in Figure 3. We focused on the peak times and landfall times of 49 typhoons. In addition, the same analysis was conducted on 20 extratropical cyclones (ECs) that occurred in 2020 to compare with the 49 typhoons. The NCEP FNL data (1 deg x 1 deg) were used to analyze the structure of the EC. In this study, extratropical cyclones corresponding to the following three conditions were defined as the target EC. 1) Extratropical cyclones do not originate from

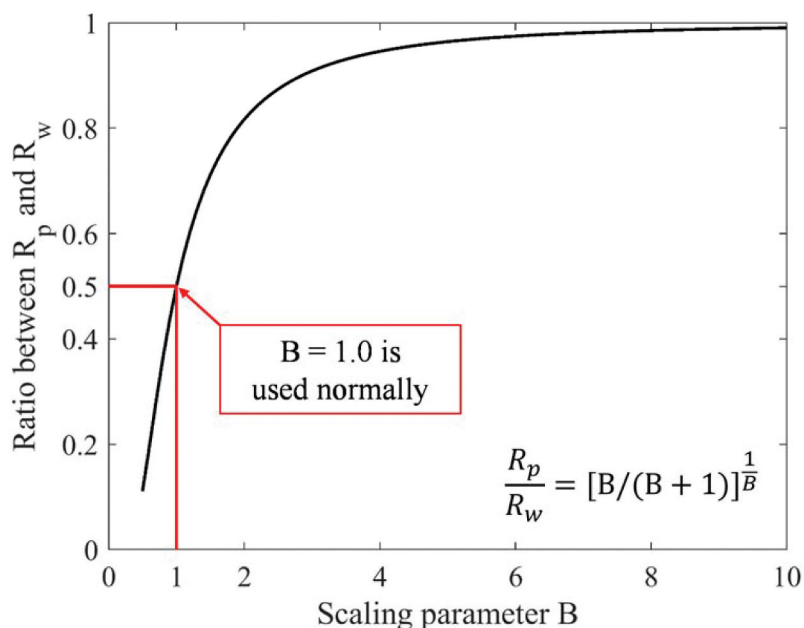


Figure 2. Relationship between Scaling parameter B and Ratio between R_p and R_w . The red arrow indicates the $B = 1$ sets used in normal empirical typhoon models.

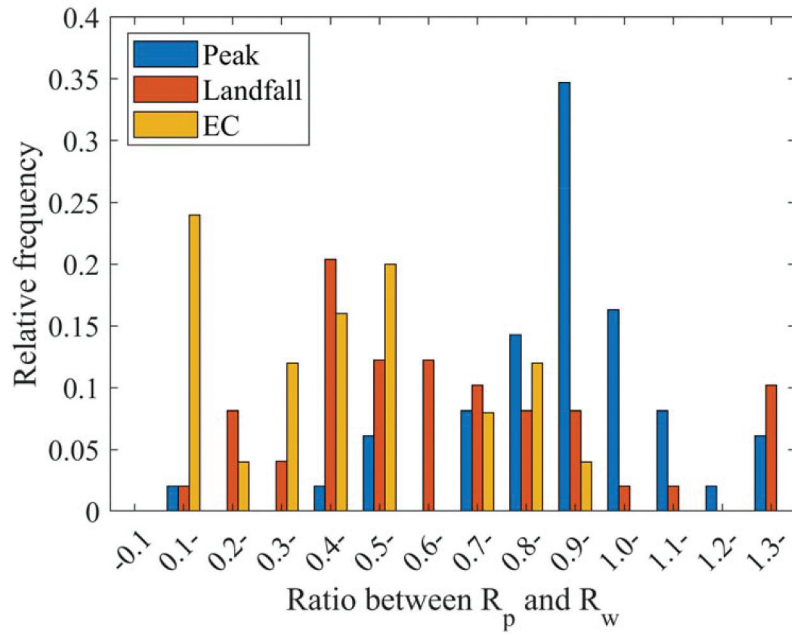


Figure 3. The distribution of Ratio between R_p and R_w in 49 typhoons. The blue bar indicates the R_p/R_w at the time of peak, the red bar indicates the R_p/R_w at the time of landfall, and the yellow bar indicates the R_p/R_w of extratropical cyclones.

typhoons. This analysis focuses on cases that have been generated and developed exclusively as extratropical cyclones. 2) Extratropical cyclones developed to less than 980 hPa are selected as targets. 3) There are no other disturbances (typhoons or extratropical cyclones less than 980 hPa) around the target. Extratropical cyclones satisfying these conditions are detected in the same area (120°–180° E, 10°–70° N), similar to the typhoon case. According to the frequency distribution, many typhoon cases show $R_p/R_w = 0.9$ at the peak time of the typhoon (blue bars in Figure 3). This result shows that R_p and R_w are almost the same at the peak time of typhoons (red bars in Figure 3). The number of cases tends to be large between 0.4 and less than 0.6 at the time of landfall (red). Approximately half of the typhoon landfall cases featured $\sim R_p/R_w = 0.5$. Hence, the fixed value of R_p/R_w (0.5) in the ETM is not an irrelevant setting. Furthermore, it cannot be ignored because each class of 0.6–1.0 has the ratio of approximately 10%. However, the R_p/R_w of the typhoon at the time of landfall varies significantly from case to case. In order to eliminate data bias, the 20 ECs are extracted with different values of minimum pressure, season, and location of occurrence. Consequently, the results vary. However, the largest class has 0.1–0.2 frequency distribution, and 75% of the total is included in the classes less than 0.6. Therefore, R_p/R_w is smaller in ECs than in typhoons. Focusing on the shape of the frequency distribution, the peak of the frequency of R_p/R_w at the peak time of the typhoon is located on the far right. In addition, the peaks of the frequency distribution move to the left in the order of the landfall times of typhoons

and ECs. Therefore, it is inferred that the value of R_p/R_w becomes smaller than the typhoon peak times, landfall times to transitioning to EC. A TC undergoing extratropical transition (ET) is denoted here as ET-TC. The widely used constant relation of the R_p/R_w by the ETM is not satisfied in the simulated TCs and can be changed from offshore to the coast due to the developing process of TC and topographical effects on TCs. The relationship between typhoon attenuation and radius requires further study.

The frequency distributions show a tendency for R_p/R_w to decrease in the order of peak intensity of typhoons, landfalls, and ECs. During landfall, R_p/R_w is smaller than that of the peak because the typhoon structure is closer to that of an EC. Here, we examine whether the typhoon tended to become an ET-TC. Whether the structure of target typhoons at the time of landfall is changing from a tropical cyclone to an ET-TC, is determined by the method proposed by Hart (2003).

$$I = h \left(\overline{Z_{600hPa} - Z_{900hPa}}|_{right} - \overline{Z_{600hPa} - Z_{900hPa}}|_{left} \right) \quad (7)$$

Here, h is 1 in the northern hemisphere and -1 in the southern hemisphere. I indicates an index of the structure of a typhoon, and Z [m] indicates the geopotential height on the isobaric surface. The right side of Equation (7) indicates the difference between the right and left averages of the layer thickness in the 600–900 hPa range. The range is within 500 km of the typhoon center relative to the direction of the disturbance movement. Hart (2003) also proposed equations

to determine whether warm or cold-core structures are an indicator of the completion of the EC structure. However, we do not use them because we intend to determine whether the transition to ET-TC has begun. The asymmetry of the thermal structure of a typhoon can be investigated using Equation (7). We use this equation to determine whether a typhoon has begun to transition into an ET-TC. According to Evans and Hart (2003), the initiation of the change from a typhoon to ET-TC is defined at $l = 10$. Note that a value $l = 10$ or more indicates the initiation of transition to an ET-TC, not its completion. The analysis results of l for 49 typhoons at the time of landfall are 33 cases (67% of the total) with over $l = 10$. In two-thirds of the cases, the symmetric structures that characterize typhoons begin to disintegrate. Hence, it is inferred that the target typhoons in this study were under the influence of conditions that facilitated the transition to ET-TC at the time of landfall in Japan. The average intensity at landfall of the 33 cases with $l \geq 10$ is 967.3 hPa, and that of the 16 cases with $l < 10$ is 959.4 hPa. There is a significant difference (one-sided t-test, significance level of 5%) between these averages. Therefore, typhoons with higher intensity at landfall are more likely to maintain their typhoon structures. Furthermore, the left-right asymmetry can also be seen in the typhoons with $l < 10$. These results indicate that most of the target typhoons in this study were in a state of ET-TC, that is, in a transitory state from a typhoon to EC, at the time of landfall in Japan.

In addition to evaluating the typhoon structure index l , vertical wind shear was confirmed. Vertical wind shear is one of the most important indicators for evaluating the maintenance of typhoon structures. The average vertical shear (200–850 hPa) around the typhoon was investigated, as shown in Figure 4.

Following Ueno and Kunii (2009) method, the vertical wind shear was calculated within 300 km of the typhoon center. Here, vertical wind shear is defined as the vector difference between the average 200-hPa, and 850-hPa winds (i.e. 200 hPa minus 850 hPa). According to previous studies (Klein, Harr, and Elsberry 2000; Davis, Jones, and Riemer 2008), it is reported that the threshold of vertical wind shear of approximately 10.0 m/s is a criterion for whether a typhoon can maintain a tropical cyclone structure. Approximately 90% of the cases demonstrated less than 10 m/s at the peak time of typhoons in the distribution of 49 typhoons (Figure 4). Cases with vertical wind shear of 5–10 m/s are the most common, followed by those with less than 5 m/s. Therefore, the winds around the typhoon were uniformly distributed, suggesting that the environment was conducive to maintaining the typhoon structure. Moreover, 67.4% were more than 10 m/s at the time of landfall. Approximately half of the cases have a vertical wind shear of 10–15 m/s, and approximately 17% have a wind shear of more than 15 m/s. In addition, vertical wind shear increased from peak time in almost all cases (44 out of 49 cases), including cases corresponding to less than 10 m/s. In approximately 78% of the cases (26 out of 33 cases) with $l \geq 10$, the vertical wind shear was also greater than 10 m/s. Therefore, these results indicate that it is an environment that is conducive to the transition from a typhoon to ET-TC at the time of landfall in Japan.

According to the analysis results of typhoon structure index l and vertical wind shear, typhoons are influenced by conditions that facilitate the transition to ET-TC. In addition, the value of R_p/R_w is expected to fluctuate significantly under these conditions. Note

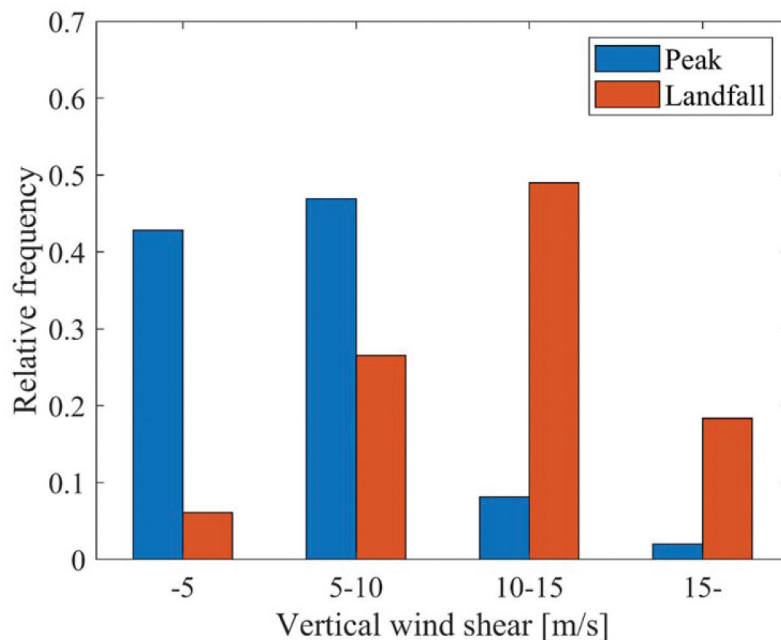


Figure 4. The distribution of vertical wind shear in 49 typhoons. The color of the bars follows Figure 2

that this analysis focuses on the time of landfall. Therefore, when and where a TC transitions into an ET-TC are not discussed here.

3.2. Relationship between typhoon attenuation and R_p/R_w

The frequency distribution in the previous section shows that R_p/R_w tends to decrease below 1 as the typhoon attenuates and approaches an ET-TC. Therefore, there could be a negative correlation between the relative weakening rate (hereafter, W_{rate} [%]) of the typhoon intensity after the peak time and R_p/R_w . Additionally, the intensity of the longer-traveled typhoon tends to decay from its peak. Hence, there could also be a negative correlation between the distance from the point where the typhoon reaches peak intensity to landfall (hereafter, D_{pl} [km]) and R_p/R_w . Note that this D_{pl} is a straight-line distance between two points, not the distance along the track of the typhoon. Although the distance along the typhoon trajectory can be used from operational forecasts, the uncertainty is exceedingly large for forecasts with long lead times. In addition, there is no information provided by the JMA for more than 120 h lead times. Therefore, in this study, we used the straight-line distance for simplicity. It is inferred that the more attenuated the typhoon (the longer the typhoon movement distance), the smaller the R_p/R_w . The W_{rate} of typhoon intensity is calculated from the following equation:

$$W_{rate} = \frac{P_{cl} - P_{cp}}{P_{cp}} \times 100 \quad (8)$$

where P_{cp} [hPa] is the central pressure at the peak times, and P_{cl} [hPa] is the central pressure at landfall times.

Figures 5 and 6 show a scatter plot of W_{rate} and R_p/R_w , and D_{pl} and R_p/R_w , respectively. These figures indicate the R_p/R_w values for typhoons at landfall. Cases with a W_{rate} of approximately zero exhibit a large variation. Moreover, R_p/R_w tends to decrease as W_{rate} increases. The correlation coefficient between R_p/R_w and the W_{rate} is -0.55 , and it can be said that the more attenuated typhoon cases tend to have smaller R_p/R_w . This can be attributed to typhoon attenuation and the disintegration of the typhoon structure. As confirmed in Section 3.1, changes to the extratropical cyclone are considered to have started at the time of landfall in many typhoon cases. In the case of extratropical cyclones, the value of R_p/R_w tends to be smaller than that of typhoons. Therefore, R_p/R_w tends to be smaller for more attenuated typhoons. Furthermore, there was also a negative correlation (-0.47) between the D_{pl} and R_p/R_w . Here, the correlation coefficient between W_{rate} and D_{pl} is 0.66 . A typhoon with a long distance to the landfall from the position of the peak intensity tends to be more attenuated. Therefore, the same relationship can be obtained for D_{pl} and R_p/R_w . Although individual variations are large, R_p/R_w tends to be smaller for typhoons that travel longer distances beyond the peak intensity. Both analyses indicate a decreasing R_p/R_w relation, from the maximum developed condition to the decay process.

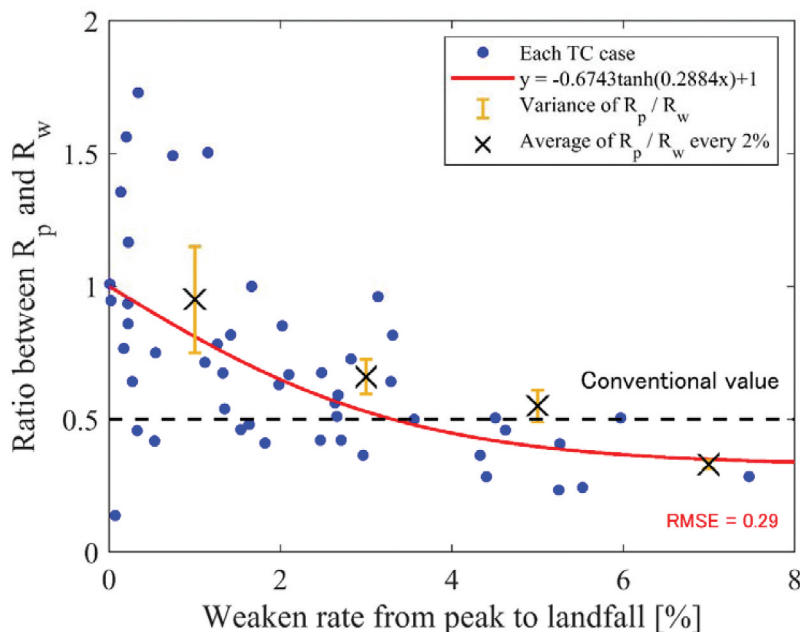


Figure 5. The relationship between weaken rate of typhoon from peak to landfall and the R_p/R_w . The blue dots mean each typhoon case (TC case). The red solid line means regression curve, error bar means variance of R_p/R_w , and the average value of R_p/R_w for every 2% (x mark) are indicated.

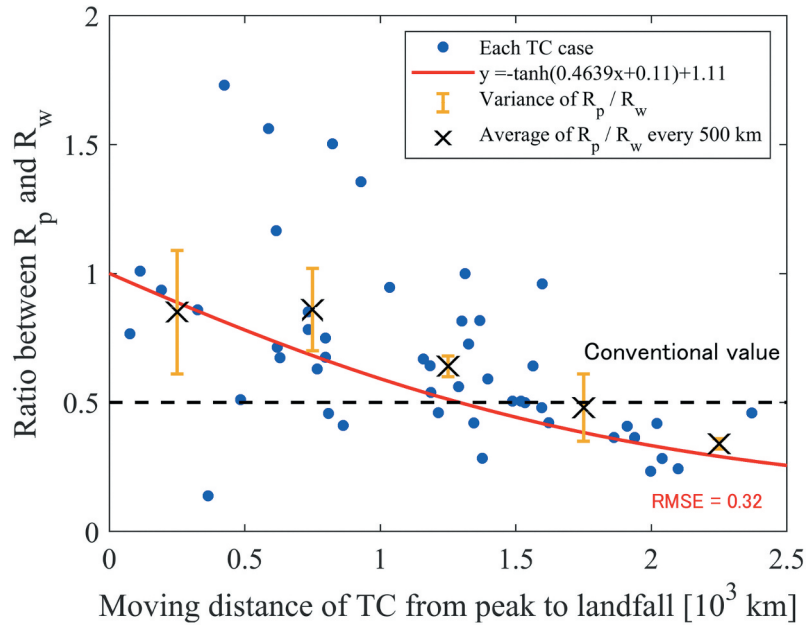


Figure 6. The relationship between the moving distance of typhoon from peak to landfall and the R_p/R_w . The blue dots mean each typhoon case (TC case). The red solid line means regression curve, error bar means variance of R_p/R_w , and the average value of R_p/R_w for every 500 km (x mark) are indicated.

4. Empirical relations of two radius based on recent typhoon cases

4.1. Estimation of R_p/R_w

It is expected that the optimization of parameter B as a function of R_p/R_w can improve the accuracy of the ETM. In the previous section, the relation of R_p/R_w was analyzed, and R_p/R_w was found to be related to the W_{rate} and D_{pl} . To evaluate the R_p/R_w of a typhoon expected to landfall in the future, the predicted W_{rate} and D_{pl} are required. In this study, we propose an empirical relation that uses the typhoon forecast values (typhoon intensity and typhoon track) provided by the Japan Meteorological Agency (JMA) to predict W_{rate} and D_{pl} . Two different empirical relations are proposed to estimate R_p/R_w as a function of W_{rate} or D_{pl} :

$$R_p/R_w = -0.6743 \times \tanh(0.2884 \times W_{rate}) + 1.0, \quad (9)$$

$$R_p/R_w = -\tanh(0.4639 \times D_{pl}/10^3 + 0.11) + 1.11 \quad (10)$$

Here, these equations are used as a robust estimation method that reduces the weight of outliers by the least-squares method because R_p/R_w varies significantly. Additionally, \tanh is determined here as the functional form considering the shape of the scatter plot, and there is no typhoon case wherein R_p/R_w is 0. The coefficients and intercept are calculated under the condition that R_p/R_w is 1 when W_{rate} or D_{pl} is 0. In Figures 5 and 6, the red lines indicate the regression lines of Equations (9) and (10), the blue points indicate each typhoon case, X-marks show the average value of R_p/R_w , and the error bars indicate the variance of R_p/R_w . The root-mean-

square error (RMSE) in Equation (9) is 0.29, and the coefficient of determination is 0.57. However, the RMSE in Equation (10) is 0.32, and the coefficient of determination is 0.51. It is expected that the accuracy of the ETM can be improved by estimating the R_p/R_w using these estimation equations and determining parameter B . JMA provides the typhoon position, intensity, a radius of wind speed of 25 m/s or more, and a radius of wind speed of 15 m/s or more. R_w is not shown in the JMA best track, although the estimated values are available in other best tracks such as IBTrACS. However, large variations were observed depending on the estimation method employed. The most significant advantage of this study is that a realistic B value can be estimated using easily available parameters, such as the amount of attenuation from the peak intensity and the distance from the peak intensity position. The proposed two equations can be operated using the input values of the typhoon intensity forecast and typhoon track forecast, respectively.

4.2. Validation of empirical TC radius estimation

The new parameter B is obtained from Equations (5), (9), and (10). In this section, the new parameter B is used to validate the improvement in the ETM. The effect of improvement using the new parameter B was validated based on three typhoon cases that severely damaged Japan in recent years (Figure 7). The typhoon cases used for validation were Toyoda, Yoshino, and Kobayashi (2018), Typhoon Faxai (2019), and Typhoon Hagibis (2019) that were not used in the evaluation of the above statistical equations. In

addition, each validation was conducted based on time series at three sites ((a) Kansai International Airport, (b) Chiba, and (c) Yokohama) where significant pressure drop and strong wind speed were observed for each typhoon (Figure 7; black line). The simulations were conducted using the information of the time when the typhoon was the closest in each case. Simultaneously, the estimation results using the conventional ETM ($B = 1$, B calculated using Equation (6)) are also shown for comparison (Figure 7; red and yellow lines). The best track of the JMA and the estimated value of R_w by satellite observation of NOAA (https://rammb-data.cira.colostate.edu/tc_realtime/) are used for the values of typhoon position, typhoon intensity, and R_w required for calculation by the ETM.

As shown in Figure 7, the accuracies were improved in some cases. The blue dashed line is the result obtained using Equation (9), and the green dashed line is the result obtained using Equation (10). At the Kansai International Airport at the time of the Jebi attack (Figure 7(a)), the parameter B is estimated as 1.12 using Equation (6), 0.850 using Equation (9), and 0.755 using Equation (10). This accurately represents the pressure until the typhoon approaches. The average estimation error of air pressure is approximately 7.0 hPa and 8.4 hPa in the setting of $B = 1$ and $B = 1.12$, respectively. However, each average error of the ETM with the new parameter B is 4.9 hPa and 3.5 hPa, respectively. Furthermore, even if the new parameter B is used, the time lag of the wind speed cannot be improved. The waveform is considerably

different from the observed value. The shape of the typhoon Jebi had already collapsed into an ellipse when Jebi reached Kansai International Airport. Therefore, the wind speed of Jebi cannot be expressed by the ETM. This problem shows the limitation of the ETM that assumes that the typhoon structure is approximated to be axisymmetric. Therefore, it is necessary to operate a dynamic model, such as a mesoscale meteorological model, to solve this problem.

In the case of Faxai (Figure 7(b)), the parameter B is estimated as 0.984 using Equation (6), 2.84 using Equation (9), and 1.61 using Equation (10). There is no significant improvement (0.24 hPa) in the pressure time series. However, the accuracy is improved significantly in the time series of the wind speed. Two peaks that are not expressed by the conventional model ($B = 1$ and $B = 0.984$) can be expressed, and it can be said that the effect of parameter B is large. The average estimation error of wind speed is approximately 4.8 m/s and 4.9 m/s in the setting of $B = 1$ and $B = 0.984$, respectively. However, the average errors in the ETM with the new parameter B are -2.1 m/s and 3.5 m/s, respectively. B needs to be set larger than 1 because Faxai made landfall immediately after reaching its peak intensity.

Finally, in the case of Hagibis (Figure 7(c)), the parameter B is estimated as 0.665 using Equation (6), 0.863 using Equation (9), and 0.711 using Equation (10). The accuracy of the air pressure and wind speed are improved. In particular, the peak of the wind speed is improved significantly. The B estimated using Equation

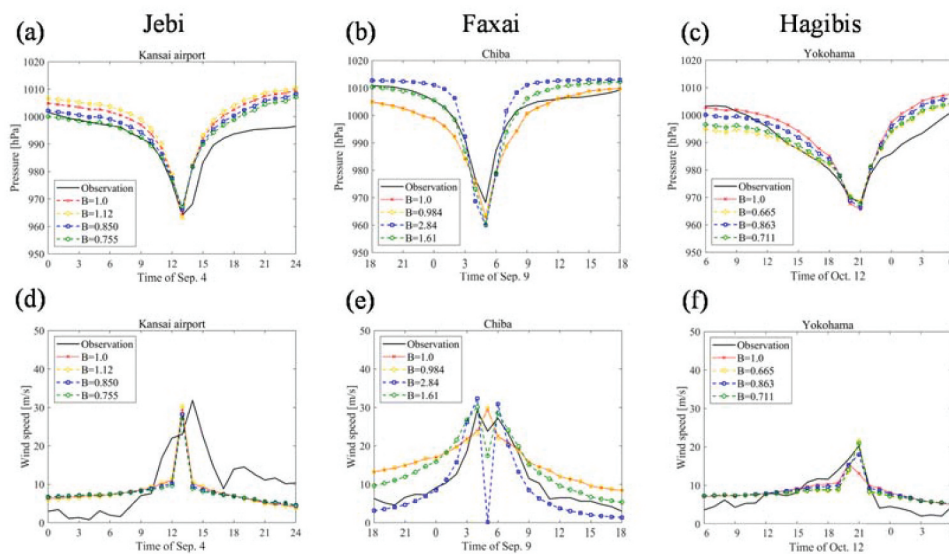


Figure 7. Time series of pressure and wind speed for selected typhoon events. Panels (a)-(c) show the pressure and the panels (d)-(f) show wind speeds. The panels (a) and (d) are results of the Kansai International Airport the case of typhoon Jebi. (b) and (e) are results of the observation site at the Chiba the case of typhoon Faxai. (c) and (f) are results of the observation site at the Yokohama the case of typhoon Hagibis (black solid line indicates observation by JMA. The red dashed line with x marks indicates the estimation with $B = 1$. The yellow dashed line with diamonds indicates the estimation with the parameter B using the estimation Equation (6). The blue dashed line with square indicates the estimation with the new parameter B using the estimation Equation (9). The green dashed line with circles indicates the estimation with the new parameter B using the estimation Equation (10).

(9) tends to be larger than that estimated using Equation (10). A larger B indicates that the typhoon is closer to its peak intensity, and thus, the pressure gradient is sharper. The three typhoon cases have different intensities and tracks. The B estimated using Equation (6) tends to be more accurate than the method that fixes $B = 1$. Furthermore the B estimated using Equations (9) and (10) are more accurate than that estimated using Equation (6), considering the changes in pressure and wind speed when the typhoons approach. The accuracy of typhoon intensity is improved by employing the novel method that determines parameter B using the constructed estimation Equations (9) or (10) and Equation (5) proposed by Holland. However, it should be noted that the statistical equations developed in this study are only applicable to typhoon landfalls exclusively on the Japanese Islands.

5. Conclusion

The ETM is widely used in the field of storm surge disaster prevention in practical use. In this study, we propose estimation equations to regulate parameter B to a suitable value for improving the accuracy of the ETM. The estimation equations for the typhoon model were constructed using the results of analysis of many typhoons. Parameter B is the ratio of the radius of the maximum pressure gradient (R_p) to the radius of the maximum wind speed (R_w). Presently parameter $B = 1$ is the setting that is widely used. By analyzing the results of studies carried out on many typhoons it is seen that parameter B tends to fluctuate significantly depending on the typhoon. There is a significant variation in the ratio R_p/R_w at the time of landfall of the typhoon. Therefore, we constructed two types of equations for the convenient estimation of R_p/R_w with the aim of calculating parameter B backwards. In one equation, R_p/R_w can be calculated using the attenuation rate of the typhoon from the time of its peak to landfall. The other method uses the distance from the position where the typhoon reaches its peak intensity to the coastline. Parameter B was calculated from the estimated R_p/R_w , and the effect on accuracy was compared with the results of the conventional ETM ($B = 1$, and B estimated by the gradient-wind equilibrium assumption). Three cases of typhoons that made landfall in Japan in recent years were selected for comparison. The value of B estimated using the gradient-wind equilibrium assumption tended to be more accurate than the method with a fixed value of $B = 1$. Furthermore, the value of parameter B calculated with our estimation equations were more accurate than that estimated by the gradient-wind equilibrium assumption in all three cases, and the improvement in the accuracy of the ETM by using our estimation equations for B was validated. The setting of $B = 1$ has been

empirically used in the ETM for storm surge disaster prevention and storm surge forecasting in Japan. It is expected that, in the future, the accuracy can be improved by using the value of B calculated backwards using the proposed estimation equations. In the future, we intend to propose a method for estimating the radius of maximum wind speed. This is required as input data for the empirical model; however, it cannot be directly determined by observation. The accuracy of the empirical model will be further improved if the change in this value, with time, can be estimated with high accuracy.

Acknowledgments

This work was supported by a JSPS Research Fellow Grant (No. 20J00218), JSPS KAKENHI Grant (No. 19H00782, 21K20447), and the Integrated Research Program for Advancing Climate Models (TOUGOU Program) Grant Number JPMXD0717935498 supported by the Ministry of Education, Culture, Sports, Science and Technology (MEXT), Japan

Disclosure statement

No potential conflict of interest was reported by the author(s).

Funding

This work was supported by the Japan society for the promotion of science [19H00782]; Japan Society for the Promotion of Science [21K20447]; ministry of education, culture, sports, science and technology [JPMXD0717935498]; Japan society for the promotion of science [20J00218].

ORCID

Masaya Toyoda  <http://orcid.org/0000-0002-7124-100X>
Nobuhito Mori  <http://orcid.org/0000-0001-9082-3235>

References

- Bister, M., and K. A. Emanuel. 1998. "Dissipative Heating and Hurricane Intensity." *Meteorology and Atmospheric Physics* 65 (3–4): 233–240. doi:10.1007/BF01030791.
- Chavas, D.R., N. Lin, and K. Emanuel. 2015. "A Model for the Complete Radial Structure of the Tropical Cyclone Wind Field. Part I: Comparison with Observed Structure." *Journal of the Atmospheric Sciences* 72 (9): 3647–3662. doi:10.1175/JAS-D-15-0014.1.
- Davis, C. A., S. C. Jones, and M. Riemer. 2008. "Hurricane Vortex Dynamics during Atlantic Extratropical Transition." *Journal of the Atmospheric Sciences* 65 (3): 714–736. doi:10.1175/2007JAS2488.1.
- Dudhia, J. 1993. "A Nonhydrostatic Version of the Penn State-NCAR Mesoscale Model: Validation Test and Simulation of an Atlantic Cyclone and Cold Front." *Monthly Weather Review* 121 (5): 1493–1513. doi:10.1175/1520-0493(1993)121<1493:ANVOTP>2.0.CO;2.

- Emanuel, K. A., C. DesAutels, C. Holloway, and R. Korty. 2004. "Environmental Control of Tropical Cyclone Intensity." *Journal of Atmospheric Science* 61 (7): 843–858. doi:10.1175/1520-0469(2004)061<0843:ECOTCI>2.0.CO;2.
- Fairall, C. W., J. D. Kepert, and G. J. Holland. 1994. "The Effect of Sea Spray on Surface Energy Transports over the Ocean." *The Global Atmosphere and Ocean System* 2: 121–142.
- Fujii, T., and Y. Mitsuta. 1986. "Simulation of Winds in Typhoons by a Stochastic Model." *J. Of Wind Engineering* 28: 1–12.
- Hart, R. E. 2003. "A Cyclone Phase Space Derived from Thermal Wind and Thermal Asymmetry." *Monthly Weather Review* 131 (4): 585–616. doi:10.1175/1520-0493(2003)131<0585:ACPSDF>2.0.CO;2.
- Holland, G. J. 1980. "An Analytic Model of the Wind and Pressure Profiles in Hurricanes." *Monthly Weather Review* 108 (8): 1212–1218. doi:10.1175/1520-0493(1980)108<1212:AAMOTW>2.0.CO;2.
- Hubbert, G. D., G. J. Holland, L. M. Leslie, and M. J. Manton. 1991. "A Real-time System for Forecasting Tropical Cyclone Storm Surges." *Weather and Forecasting* 6 (1): 86–97. doi:10.1175/1520-0434(1991)006<0086:ARTSFF>2.0.CO;2.
- Jelesnianski, C., J. Chen, and W. Shaffer. 1992. "SLOSH: Sea, Lake, and Overland Surges from Hurricanes." In *NOAA Technical Report NWS Vol. 48*. Silver Spring, MD:United States Department of Commerce, NOAA, NWS, 71 .
- Kawasaki K., S. Shimokawa, and T. Murakami. (2016) "Storm surge inundation prediction due to huge typhoon at head of Ise Bay". *JSCE B2 (Coastal Engineering)*. 72 (2): 211–216.
- Klein, P. M., P.A. Harr, and R. L. Elsberry. 2000. "Extratropical Transition of Western North Pacific Tropical Cyclones: An Overview and Conceptual Model of the Transformation Stage." *Weather and Forecasting* 15 (4): 373–396. doi:10.1175/1520-0434(2000)015<0373:ETOWNP>2.0.CO;2.
- Matoba, M., K. Murakami, and H. Shibaki. 2006. "Super Gradient Wind (SGW) Based Typhoon Wind Estimation and Storm Surge Simulation." *Journal of Japan Society of Civil Engineers, Series B2 (Coastal Engineering)* 53: 206–210. doi:10.2208/proce1989.53.206.
- Ministry of Land, Infrastructure, Transport and Tourism, Japan. 2020. "Storm Surge Inundation Assumption Area Figure Making Manual (Ver.2.00)." 84.
- Mori, N., M. Kato, S. Kim, H. Mase, Y. Shibutani, T. Takemi, K. Tsuboki, and T. Yasuda. 2014. "Local Amplification of Storm Surge by Super Typhoon Haiyan in Leyte Gulf." *Geophysical Research Letters* 41 (14): 5106–5113. doi:10.1002/2014GL060689.
- Murakami, T., T. Yasuda, and J. Yoshino. 2007. "Reproduction of Storm Surge Generated by Typhoon 0416 over a Large Area Using Meteorological Model and Multi-sigma Coordinate Ocean Model." *Journal of Japan Society of Civil Engineers, Series B2 (Coastal Engineering)* 63 (4): 282–290. doi:10.2208/jscejb.63.282.
- Myers, V. A. 1954. "Characteristics of United States Hurricanes Pertinent to Levee Design for Lake Okeechobee, Florida." *Hydrometeorological Report, U.S Weather Bureau* 32, 126.
- Schloemer, R.W. 1954. "Analysis and Synthesis of Hurricane Wind Patterns over Lake Okeechobee, Florida." *Hydrometeorological Report* 31: 49.
- Shade, L. R., and K. A. Emanuel. 1999. "The Ocean's Effect on the Intensity of Tropical Cyclones: Results from a Simple Coupled Atmosphere-Ocean Model." *Journal of Atmospheric Sciences* 56 (4): 642–651. doi:10.1175/1520-0469(1999)056<0642:TOSEOT>2.0.CO;2.
- Shibutani Y., N. Mori, S. Kim, S. Nakajyo, and H. Mase, 2017. "Sensitivity analysis of storm surge height and inundation area around Tokyo Bay by changing typhoon characteristics due to climate change". *JSCE B2 (Coastal Engineering)* 73 (2): 1399–1404.
- Skamarock, W. C., J. B. Klemp, J. Dudhia, D. O. Gill, D. M. Barker, M. G. Duda, X-Y. Huang, W. Wang, and J. G. Powers. 2008. "A Description of the Advanced Research WRF Version 3." In *NCAR Tech. Note*. Boulder, Colo: **475** 113 National Center for Atmospheric Research, 125.
- Toyoda, M., J. Yoshino, and T. Kobayashi. 2018. "Statistical Characteristics on Future Changes of the Intensity of Typhoons Landfalling in the Main Islands of Japan." *Journal of Japan Society of Civil Engineers, Series B2 (Coastal Engineering)* 74 (2): 1339–1344. (in Japanese). doi:10.2208/kaigan.74.1_1339.
- Tsuboki K., and Sakakibara A. 2002. Large-Scale Parallel Computing of Cloud Resolving Storm Simulator High Performance Computing. ISHPC 2002. Lecture Notes in Computer Science. In: Zima H.P., Joe K., Sato M., Seo Y., and Shimasaki M. (eds) , vol 2327. Berlin, Heidelberg: Springer. doi:10.1007/3-540-47847-7_21.
- Ueno, M., and M. Kunii, 2009. "Some aspects of azimuthal wavenumber-one structure of typhoon represented in the JMA operational mesoscale analyses". *Journal of the Meteorological Society of Japan* 87 (4): 615–633.
- Vickery, P. J., and D. Wadhera. 2008. "Statistical Models of Holland Pressure Profile Parameter and Radius to Maximum Winds of Hurricanes from Flight-level Pressure and H*Wind Data." *Journal of Applied Meteorology and Climatology* 47 (10): 2497–2517. doi:10.1175/2008JAMC1837.1.
- Wang, Y., J. D. Kepert, and G. J. Holland. 2001. "The Effect of Sea Spray Evaporation on Tropical Cyclone Boundary Layer Structure and Intensity." *Monthly Weather Review* 129 (10): 2481–2500. doi:10.1175/1520-0493(2001)129<2481:TEOSSE>2.0.CO;2.
- Wang, S., R. Toumi, A. Czaja, and A.V. Kan. 2015. "An Analytic Model of Tropical Cyclone Wind Profiles." *Quarterly Journal of the Royal Meteorological Society* 141 (693): 3018–3029. doi:10.1002/qj.2586.
- Willoughby, H. E., R. W. R. Darling, and M. E. Rahn. 2006. "Parametric Representation of the Primary Hurricane Vortex. Part II: A New Family of Sectionally Continuous Profiles." *Monthly Weather Review* 134 (4): 1102–1120. doi:10.1175/MWR3106.1.
- Yamaguchi, M., H. Nonaka, M. Hino, and Y. Hatada. 2012. "Investigating Occurrence Possibility of Abnormally Strong Wind Estimated Using Width Records of Resin Freckle Left along Annual Rings of YAKUSUGI." *Journal of Japan Society of Civil Engineers, Series B1 (Hydraulic Engineering)* 68 (4): 1-1675-1680. doi:10.2208/jscejhe.68.1_1675.
- Zhang, D. L., and E. Altshuler. 1999. "The Effects of Dissipative Heating on Hurricane Intensity." *Monthly Weather Review* 127 (12): 3032–3038. doi:10.1175/1520-0493(1999)127<3032:TEODHO>2.0.CO;2.